Search for the violation of time-reversal invariance in $K^0_{\mu 3}$ decays

W. M. Morse, L. B. Leipuner, and R. C. Larsen
Brookhaven National Laboratory, Upton, New York 11973

M. P. Schmidt,* S. R. Blatt, M. K. Campbell, D. M. Grannan, M. J. Lauterbach, H. Kasha, and R. K. Adair
Yale University, New Haven, Connecticut 06520

(Received 11 October 1979)

The transverse polarization of muons from the decay $K^0_L \to \pi^- \mu^+ \nu_\mu$ has been recently measured at Brookhaven National Laboratory. A cylindrically symmetric detector was employed with scintillation-counter hodoscopes detecting the charged decay products of the in-flight kaon decay and determining the orientation of the decay plane in the laboratory. Muons were brought to rest in an aluminum polarimeter where they precessed in 60-G magnetic field. The muon polarization was determined from the asymmetric emission of the positron in the muon decay ($\mu^+ \to e^+ \nu_e \bar{\nu}_\mu$). With 12×10^6 events collected the mean values measured for the two components of transverse polarization are $P_n^{\text{lab}} = 0.0017 \pm 0.0056$ for the component normal to the decay plane and $P_t^{\text{lab}} = 0.417 \pm 0.063$ for the component in the decay plane. For Imξ, where ξ is the ratio of form factors describing $K_{\mu 3}$ decay, we have deduced a value of 0.009 ± 0.030 which is not significantly different from the value 0.008, expected if time-reversal invariance is valid. We deduce that the average value of the ratio of the normal to transverse components of muon polarization in the kaon rest frame is given by $\langle P_n/P_t \rangle^{\text{c.m.}} = 0.005 \pm 0.015$.

I. INTRODUCTION

It has been known for some time that CP invariance is not an exact symmetry of nature.[1] To date, CP violation has been observed only in the decay systematics of the K^0-$\bar{K}^0$ complex where a parameter defining the violation has been carefully measured.[2] Such observations are consistent with a superweak[3] model of CP violation in which a first-order $|\Delta S| = 2$ interaction of strength $\sim 10^{-9} G_F$ is responsible for the CP impurity of the K^0_L (K^0_S) state. The effects observed in the K^0-$\bar{K}^0$ system are then described in terms of one parameter: the ratio of the CP-allowed and -forbidden amplitudes for the decays of neutral kaons into two pions, $\epsilon = |\text{Amp}(K^0_L \to 2\pi)/\text{Amp}(K^0_S \to 2\pi)| \cong 2.3 \times 10^{-3}$. Because the superweak interaction is weaker than the weak interaction in second order, CP-violating effects outside of the K^0-$\bar{K}^0$ system are expected to be unobservable with present techniques.

However, it is possible that the mechanism of CP violation is milliweak in character with the violation occurring directly, in the sense that the transition ($K^0_L \to 2\pi$) occurs from a CP pure state, through an interaction of strength $10^{-3} G_F$. Milliweak models of CP violation are able to reproduce, with small deviations, the superweak predictions for the K^0-$\bar{K}^0$ system, and in addition predict CP-violating effects on the order of 10^{-3} outside the K^0-$\bar{K}^0$ system.

In this regard, searches for a direct violation of time-reversal invariance (T) are of great interest. Given the observed violation of CP invariance and the assumption of CPT invariance, a corresponding T violation is expected. In fact, detailed studies of the K^0-$\bar{K}^0$ system imply T violation and CPT invariance.[4] However, previous searches for a direct T-violating effect, for instance in an electric dipole moment for the neutron,[5] in a nuclear polarization normal to the decay plane in nuclear β decay,[6] and in a muon polarization normal to the decay plane in $K_{\mu 3}$ decay[7] have yielded negative results. At the same time these efforts have set the most stringent limits on CP violation outside of the K^0-$\bar{K}^0$ system, and may yet serve to decide between superweak and milliweak models of CP violation.

Recently, with the apparent success of gauge theories in unifying the weak, the electromagnetic, and possibly the strong interactions, interest in CP violation has been renewed in the hope that it can be incorporated naturally in this framework. It is possible to generate CP violation in the context of gauge theories by including genuine complex phases in the weak transitions of quarks. However, the standard four-quark SU(2) × U(1) model of the weak and the electromagnetic interactions must be modified in order to obtain such observable phases.[8] We know of three possible gauge-theory realizations of CP violation.

The first mechanism involves right-handed as well as left-handed currents in the weak quark transitions, and CP violation is the result of a complex phase in the interference between these currents. Models based on this mechanism can be constructed to yield superweak or milliweak results for CP violation. At this time though, no evidence for right-handed currents exists.[9]

The discovery of a new lepton τ,[10] and of evidence for a new quark b, in the Υ,[11] has renewed interest in the six-quark extension of the standard SU(2) × U(1) model, due to Kobayashi and Maskawa.[12] They have shown that an irreducible complex phase appears in the gauge couplings of the quarks when the standard model is extended from two to three left-handed quark doublets. In principle the magnitude of CP violation is arbitrary in such models. However, once parameters are adjusted to yield CP violation as observed in the K^0-$\bar{K}^0$ system, the predictions are close to[13] superweak in nature. No easily observable effects are predicted outside the K^0-$\bar{K}^0$ system and estimates[14] for the electric dipole of the neturon yield values $D_n^e \lesssim 10^{-30}$ e cm, well below the present experimental limits of $D_n^e \lesssim 3\times 10^{-24}$ e cm.[5]

A third mechanism of CP violation has been suggested by Weinberg.[15] In an otherwise standard four-quark SU(2) × U(1) model, CP violation is spontaneously generated and confined to an enlarged Higgs sector. A natural explanation for the smallness of CP violation is then given by the relatively large masses of the Higgs particles ($\gtrsim$15 MeV). The predictions are milliweak in nature with an expected[15,16] value for the neutron electric dipole moment of $D_n^e \sim 10^{-24}$ to 10^{-25} e cm which is just compatible with the current experimental limits. Although detailed calculations are not available, Higgs-particle-mediated CP-violating effects are expected to be on the order of 10^{-3} in $K_{\mu 3}$ decays but vanishingly small in nuclear β decay. This result follows from the nature of the Higgs-particle–quark couplings which are proportional to the quark mass. With more than four quarks, such models seem less attractive, but the possibility remains that CP violation has more than one source.

As suggested by the theoretical efforts mentioned above, further improvements in the limits set on CP-violating processes outside of the K^0-$\bar{K}^0$ system will be fundamental in reaching an understanding of the nature of CP violation. The present limits for the electric dipole moment of the neutron approach the sensitivity required to rule out a large class of milliweak models of CP violation, and the results from nuclear β-decay measurements are almost that sensitive if light-quark (u and d) transitions are important in CP violation. However, previous measurements of muon polarization in $K_{\mu 3}$ decays have not been so precise. In a recent paper[17] we have reported results extending the sensitivity of measurements on the component of polarization normal to the decay plane in the decay $K_L^0 \to \pi^- \mu^+ \nu_\mu$. This measurement is the first of a program designed to achieve the sensitivity required to detect the milliweak CP-violating effect expected if transitions involving strange quarks are especially important.

In the following, after a brief review of the phenomenology of $K_{\mu 3}$ decays, we describe in some detail the apparatus used in our measurements. Details of the analysis are presented and the results are discussed.

II. PHENOMENOLOGY

A. $K_{\mu 3}$ decay

The decay $K_L^0 \to \pi^- \mu^+ \nu_\mu$ is described by the matrix element[18]:

$$M = \frac{G_F}{\sqrt{2}} \sin\theta_C \langle \pi^- | J_\lambda^1 | K_L^0 \rangle \bar{u}_{\nu_\mu} \gamma^\lambda (1+\gamma^5) v_\mu ,$$

where J_λ^1 is the strangeness-changing ($|\Delta S| = 1$, $\Delta S = \Delta Q$) part of the weak hadronic current. J_λ^1 is a vector current as required by the 0^- spin-parity of the pion and the kaon, and the assumed local $V-A$ structure of the leptonic current. No evidence for the more generally allowed scalar and tensor couplings has been detected in previous experiments.[19]

Lorentz invariance and energy-momentum conservation require that the four-vector current $\langle \pi^- | J_\lambda^1 | K_L^0 \rangle$ depends only on the two independent four-vector momenta describing the hadronic vertex and the nontrivial Lorentz scalar formed from them. A parametrization traditionally chosen is

$$\langle \pi^- | J_\lambda^1 | K_L^0 \rangle = f_+(q^2)(p_K + p_\pi)_\lambda + f_-(q^2)(p_K - p_\pi)_\lambda ,$$

where $q^2 = (p_K - p_\pi)^2$ is the square of the four-momentum transferred to the leptonic current, and $f_\pm$ are form factors containing the structure of the hadronic vertex due to the strong interactions.

In general the functions f_+ and f_- are complex, but time-reversal invariance requires such coherently interferring amplitudes to be relatively real.[20] With the definition $\xi(q^2) = f_-(q^2)/f_+(q^2)$, the hadronic current may be rewritten as

$$\langle \pi^- | J_\lambda^1 | K_L^0 \rangle = f_+(q^2)[(p_K + p_\pi)_\lambda + \xi(q^2)(p_K - p_\pi)_\lambda] ,$$

and it is apparent that a nonvanishing value for $\mathrm{Im}\,\xi(q^2)$ indicates a violation of time-reversal invariance. It is also noted that, by use of the Dirac equation, the matrix element may be reexpressed as

$$M = \frac{G_F}{\sqrt{2}} \sin\theta_C f_+(q^2)\{2p_K^\lambda \bar{u}_{\nu_\mu} \gamma_\lambda (1+\gamma^5) v_\mu + m_\mu [\xi(q^2) - 1] \bar{u}_{\nu_\mu} (1-\gamma^5) v_\mu\} .$$

In the kaon rest frame the term involving $(\xi - 1)$ is proportional to m_μ / m_K. Clearly then, the systematics of K_{e3} decays are insensitive to ξ as $m_e/$

$m_K \ll 1$.

The dependence of the muon polarization in $K_{\mu 3}$ decays on $\xi(q^2)$ has been calculated by MacDowell[21] and by Cabibbo and Maksymowicz.[22] In laboratory coordinates the muon polarization is expressed as

$$\hat{S}_\mu^{\rm lab} = \vec{B}/|\vec{B}|,$$

where

$$\vec{B} = b_1(\xi)\left[\left(\frac{\vec{p}_\mu}{m_\mu}\right)\left(\frac{\vec{p}_\nu\cdot\vec{p}_\mu}{E_\mu+m_\mu} - E_\nu\right) + \vec{p}_\nu\right] + b_2(\xi)\left[\left(\frac{\vec{p}_\mu}{m_\mu}\right)\left(\frac{\vec{p}_K\cdot\vec{p}_\mu}{E_\mu+m_\mu} - E_K\right) + \vec{p}_K\right]$$
$$-(\mathrm{Im}\,\xi)\left[E_K(\vec{p}_\mu\times\vec{p}_\pi) + E_\mu(\vec{p}_\pi\times\vec{p}_K) + E_\pi(\vec{p}_K\times\vec{p}_\mu) + \frac{\vec{p}_\mu\cdot(\vec{p}_K\times\vec{p}_\pi)}{E_\mu+m_\mu}\vec{p}_\mu\right],$$

with

$$b_1(\xi) = m_K^2 + m_\mu^2|b(q^2)|^2 + 2[\mathrm{Re}\,b(q^2)](p_\mu\cdot p_K),$$
$$b_2(\xi) = -2(p_\nu\cdot p_K) - [\mathrm{Re}\,b(q^2)](q^2 - m_\mu^2),$$

and

$$b(q^2) = \tfrac{1}{2}[\xi(q^2) - 1];$$

also $p_a\cdot p_b = E_aE_b - \vec{p}_a\cdot\vec{p}_b$. In the kaon rest frame, obtained by taking $\vec{p}_K = 0$ and $E_K = m_K$, it is apparent that the T-violating polarization is proportional to $(\mathrm{Im}\,\xi)m_K(\vec{p}_\pi\times\vec{p}_\mu)$, and thus time-reversal invariance requires a vanishing muon polarization normal to the decay plane.

However, it is important to note that in the decay $K_L^0 \to \pi^-\mu^+\nu_\mu$, CP-invariant electromagnetic final-state interactions induce a pseudo-T-violating effect. The interference between amplitudes with and without a virtual photon exchange between the outgoing pion and muon has been calculated[23] to produce a nonzero value for $\mathrm{Im}\,\xi$:

$$\mathrm{Im}\,\xi|_{\rm em} \cong \frac{e^2}{4\pi}\frac{m_\pi^2 + (p_\pi\cdot p_\mu)}{[(p_\pi\cdot p_\mu)^2 - m_\pi^2 m_\mu^2]^{1/2}} \times\left[1 - \frac{1}{4}\frac{m_\mu^2|1-\xi|^2}{(p_\pi+p_\mu)^2}\right],$$

which is typically of the order 0.008. The effects of final-state interactions are not negligible in an experiment achieving a precision in $\mathrm{Im}\,\xi$ on the order of 0.01.

Insight into the dependence of the muon polarization on $\xi(q^2)$ is obtained by considering an alternate pair of independent amplitudes to describe $K_{\mu 3}$ decay. Specifically, if we define

$$f_0(q^2) \equiv f_+(q^2) + f_-(q^2)q^2/(m_K^2 - m_\pi^2)$$

and consider the decay in the rest frame of the lepton pair, then it can be shown[20] that $f_+(q^2)$ and $f_0(q^2)$ describe the amplitudes for the decay in which the spin-parity of the lepton pair is 1^- and 0^+, respectively. From the above definition we find that

$$f_0(q^2)/f_+(q^2) = 1 + \xi(q^2)q^2/(m_K^2 - m_\pi^2),$$

and thus $\xi(q^2)$ determines the relative amplitudes of the 0^+ and 1^- transitions.

In addition, because of the constrained helicity of the muon neutrino, the 1^- and 0^+ transitions involve a muon (μ^+) helicity of +1 and −1, respectively. This suggests that in the kaon rest frame it is possible to describe $K_{\mu 3}$ decays in terms of two amplitudes: A_u for positive muon helicity and A_d for negative muon helicity. It then follows that the transverse polarization of the muon in the decay plane will be

$$P_t = 2\,\mathrm{Re}(A_u^*A_d)/(A_u^2 + A_d^2)$$

and the component of polarization normal to the plane will be

$$P_n = 2\,\mathrm{Im}(A_u^*A_d)/(A_u^2 + A_d^2).$$

Then

$$P_n/P_t = \mathrm{Im}(A_u^*A_d)/\mathrm{Re}(A_u^*A_d) = \tan\phi,$$

where we have taken A_d to be real and $A_u = |A_u|e^{i\phi}$. The angle ϕ is the complex phase between the two interfering amplitudes. If CP violation is milliweak in character, we expect ϕ to be on the order of the CP-violating parameter ϵ.

A formal relation between ϕ and $\mathrm{Im}\,\xi$ is possible. Working in the kaon rest frame the muon polarization is rewritten in terms of components along the orthogonal set of axes:

$$\hat{n}_l = \frac{\vec{p}_\mu}{|\vec{p}_\mu|}, \quad \hat{n}_n = \frac{\vec{p}_\pi\times\vec{p}_\mu}{|\vec{p}_\pi\times\vec{p}_\mu|}, \quad \hat{n}_t = \hat{n}_l\times\hat{n}_n.$$

Then,

$$\left(\frac{P_n}{P_t}\right)^{\rm c.m.} = \frac{|\vec{p}_\pi||\vec{p}_\mu|m_K(\mathrm{Im}\,\xi)\sin\theta_{\pi\mu}}{-b_1(\xi)|\vec{p}_\pi|\sin\theta_{\pi\mu}}$$
$$= \frac{-|\vec{p}_\mu|m_K\,\mathrm{Im}\,\xi}{m_K^2 + m_K E_\mu(\mathrm{Re}\,\xi - 1) + (m_\mu^2/4)|\xi-1|^2}$$
$$= \frac{-\beta_\mu\gamma_\mu\,\mathrm{Im}\,\xi}{m_K/m_\mu + \gamma_\mu(\mathrm{Re}\,\xi - 1) + (m_\mu/4m_K)|\xi-1|^2}.$$

Here $\theta_{\pi\mu}$ is the angle between the pion and muon and $\gamma_\mu = 1/(1-\beta_\mu^2)^{1/2}$ with $\beta_\mu = |\vec{p}_\mu|/E_\mu$.

B. Experimental sensitivity

Previous measurements of the transverse polarization of muons in $K_{\mu 3}^0$ decay have set pro-

gressively more stringent limits on $\mathrm{Im}\xi$.[7,24] The experiment of Sandweiss *et al.*[7] was the most significant with 2×10^6 events and a quoted value of $\mathrm{Im}\xi = -0.060 \pm 0.045$. As in the present experiment, the method of imposed spin precession was employed, and great care was taken to design a detector relatively free from systematic errors that could give rise to a spurious T-violating effect.[25] However, it is noted that Sandweiss *et al.* measured a value of $\mathrm{Re}\xi = -0.655 \pm 0.127$ and used this value in calculations leading to the quoted value for $\mathrm{Im}\xi$. More recent precise measurements[26] indicate that $\mathrm{Re}\xi \simeq 0$, and we estimate their adjusted result to be $\mathrm{Im}\xi = -0.085 \pm 0.064$.

The sensitivity of measurements on muon polarization in $K_{\mu3}$ decays is largely determined by the experimental acceptance across the Dalitz plot. In the kaon rest frame the $K_{\mu3}$ decay configuration is completely described in terms of two variables, usually taken to be the kinetic energy of the pion and muon, T_π and T_μ. The probability density for the decay configurations is found to vary with the position on the Dalitz plot, as illustrated in Fig. 1. Also shown is the variation of the T-violating polarization P_n expected for $\xi = 0.0 + i0.01$. The maximum value of P_n found on the Dalitz plot is $P_n^{\max} = 0.43\%$ and the average value over the Dalitz plot is $\langle P_n^{\mathrm{c.m.}} \rangle = 0.21\%$. The present experiment was designed to achieve a high sensitivity in the measurement of $\mathrm{Im}\xi$. Monte Carlo calculations, including the production spectrum of the kaon beam and acceptance of the detector, determined the decay configurations in the laboratory most sensitive to $\mathrm{Im}\xi$. Averaged over the Dalitz plot the event selection then yielded $\langle P_n^{\mathrm{c.m.}} \rangle = 0.29\%$ for the canonical $\xi = 0.0 + i0.01$.

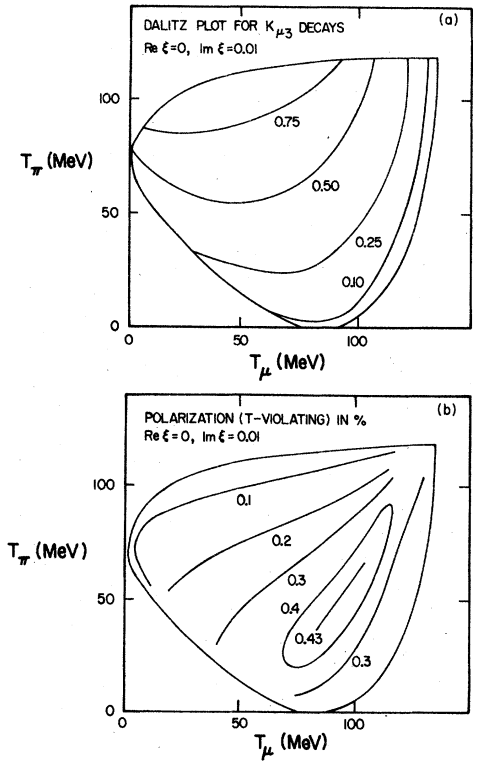

FIG. 1. (a) Contours of relative intensity for $K_{\mu3}^0$ decays on the Dalitz plot where the maximum intensity is 1.0. (b) Contours indicating the variation of the (T-violating) transverse polarization (in %) of the muon in $K_{\mu3}^0$ decays. Average value over the Dalitz plot is $\langle P_n \rangle = 0.21\%$.

III. APPARATUS

A. Introduction to the detector and the experimental technique

The apparatus consisted of a cylindrically symmetric detector centered on the axis of a neutral beam. A perspective view of the main components of the detector is shown in Fig. 2. In a typical event the charged products from the in-flight decay $K_L^0 \to \pi^- \mu^+ \nu_\mu$ were detected by the primary (π-μ) scintillation-counter hodoscope arrays (A, B, C, D, E). The muon was partially identified by hits in the counters A or B, M, and F that defined a trajectory which passed through the steel toroidal magnet and was focused into the aluminum polarimeter. The muon identification was confirmed by the detection of the electronic decay $\mu^+ \to e^+ \nu_e \bar{\nu}_\mu$ within a few microseconds of the muon coming to rest in the polarimeter.

In order to detect the T-violating correlation $\vec{S}_\mu^* \cdot (\vec{p}_\pi^* \times \vec{p}_\mu^*)$, that is, the component of muon polarization normal to the decay plane in the kaon rest frame, events were selected such that the laboratory momentum of the kaon was very nearly in the decay plane. The event selection was based

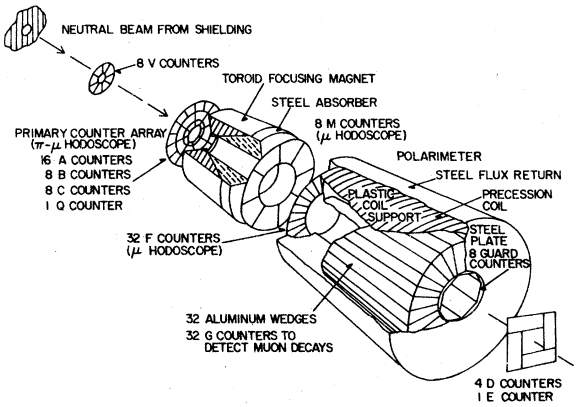

FIG. 2. An isometric view of the experimental apparatus indicating the major components of the detector. Dimensions are given in the text and in Fig. 6.

on the pattern of hits recorded in the π-μ hodoscope, and the assumption that the decay vertex was along the beam line. On the average the decay planes, as defined in the laboratory and kaon rest frames, were nearly identical, and thus the T-violating correlation measured in the laboratory was $\vec{S}_\mu \cdot (\vec{p}_K \times \vec{p}_\mu)$. Monte Carlo calculations, including the geometry and acceptance of the detector, determined the detailed event selection criteria. However, the selected events separate naturally into two qualitatively distinct classes which are discussed below.

Figure 3(a) illustrates possible decay-product orientations, as seen in the kaon rest frame and the laboratory system, which contribute to the first class (P) of events. The decay plane is unambiguously defined in either reference frame by the requirement that the pion momentum be nearly parallel to that of the kaon. The sense of the T-violating polarization is then preserved in the Lorentz transformation from the rest frame to the laboratory. Detailed calculations show that the steepness of the kaon production spectrum, and the finite transverse momentum acceptance of the pion counters along the beam line cause the event selection to be strongly biased toward those events with the pion emitted forward in the rest frame. This yields a net T-violating component of polarization which defines a clockwise screw sense about the beam line.

Similarly, Fig. 3(b) illustrates the decay product orientations typical in the second class (M) of

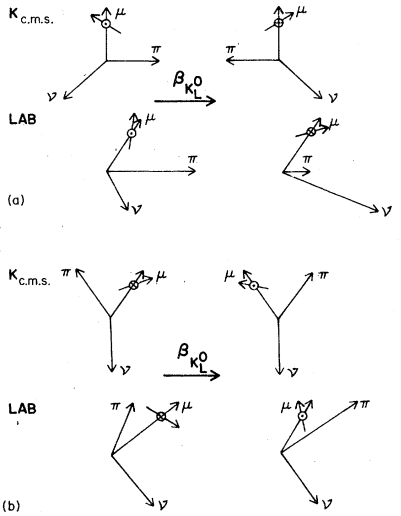

FIG. 3. (a) Orientations of the decay products and the muon polarization in the kaon rest frame and the laboratory system for a typical P class event. (b) Orientations of the decay products and the muon polarization in the kaon rest frame and the laboratory system for a typical class M event.

events. The decay plane is defined by requiring both the pion and the muon to have substantial transverse momenta, and that the projections of these momenta onto a plane normal to the beam line lie near each other in azimuthal angle about the beam line. Because of the steepness of the kaon spectrum and the energy required for the muon to penetrate the toroid, events where the muon has a larger laboratory momentum than the pion are preferentially selected yielding a net polarization. In this second class of events the net sense of the polarization is counterclockwise, providing a useful check against spurious results.

For the idealized events discussed above, the polarization of the muon in the laboratory is described in terms of components P_L, P_t, and P_n which lie along three mutually orthogonal axes. The longitudinal component P_L is parallel to the muon momentum $\vec{p}_\mu$ while P_t and P_n are the components transverse to the muon momentum with P_t lying in the decay plane $(\vec{p}_K \times \vec{p}_\mu)$, and P_n being normal to the decay plane. After passage through the toroid, the muon momentum was on the average parallel to the beam line so that for muons stopping in the polarimeter, P_L was along the beam axis, P_t was radially normal to the beam axis, and P_n was normal to a plane containing the beam axis. The component P_n is the T-violating polarization.

The geometry of the polarimeter was such that the two components of polarization, P_t and P_n, were analyzed. Figure 4(a) illustrates schematically the polarization components for a muon at rest in one of the aluminum plates of the polarimeter. The plate is flanked by two counters (U, D), and the plate and the counters lie in planes emanating radially from the beam line. The components of polarization were analyzed by studying the asymmetry $A = (U - D)/(U + D)$ in the detection of positrons in the flanking counters, as a function of time, while the muons precessed in a 60-G magnetic field. The field was directed either parallel

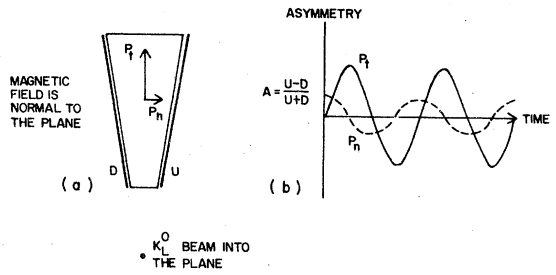

FIG. 4. (a) Schematic representation of the components of muon polarization in the polarimeter as seen along the beam line. (b) Schematic representation of the contributions of the transverse polarizations to the asymmetry for an ensemble of precessing muons.

or antiparallel to the beam line so that the muon spin precessed about this axis. For an ensemble of muons, the asymmetry A varies sinusoidally in time, as shown in Fig. 4(b), which illustrates the contributions to A from P_t and P_n. The P_t contribution which behaves as $\sin\omega t$, where ω is the precession frequency, changes sign under a reversal of the magnetic field direction. The P_n contribution which behaves as $\cos\omega t$ is not affected by the field reversal. Thus by reversing the direction of the field every pulse, the data could be analyzed so that P_t and P_n could be determined without mutual contamination. This is especially important for the determination of a small component P_n in the presence of the large P_t component ($P_t/P_n \gtrsim 300$).

B. Neutral beam

The neutral beam was produced by the interactions of 28.5-GeV/c protons with a 10.2-cm-long platinum target. With a production angle of 6°, the neutral beam was defined by a series of collimators passing through shielding walls and sweeping magnets (Fig. 5). An acceptance of approximately 10^{-4} sr was obtained by a defining aperture, 6 cm in diameter, 4.6 m from the target.

At a distance of 7 m from the target, the neutral beam passed into the detector cave and traveled through a helium filled bag to a lead and uranium beam stop downstream of the detector. As measured by a secondary-emission monitor upstream of the target, typically 6×10^{10} protons per pulse were directed onto the target, generating roughly 2×10^{6} K_L^0's in the neutral beam. The neutron flux in the beam was estimated to be a factor of 3 to 5 times larger than the K_L^0 flux. These estimates were in reasonable agreement with conversion measurements made in the beam line.

C. Decay zone

The detector was designed to accept K_L^0 decays occurring along the beam line in the first 5 m of the detector cave. Scintillation-counter arrays (Fig. 6) defined the allowed paths for the charged decay products. The large arrays, AC and K, were used in anticoincidence to reject charged particles originating upstream of the shielding wall, especially muons from the target region. A concrete wall was placed between the AC and K-V arrays to attenuate the slower neutron flux from the shielding. This wall was made with a conical hole, set by the aperture of the neutral beam pipe and the outer diameter of the V array, in order to provide unobstructed trajectories from the beam line to the detector.

The primary hodoscope arrays (A, B, C, D, E, Q, and V) were used to detect $K_{\mu3}$ decay products, and to provide information necessary for event selection. The expectation of observing two charged decay products was enforced by requiring a coincidence between two distinct A, B, C, D, and E counters. In addition to facilitating the selection of events, the segmentation of the arrays resulted in a strong reduction of various backgrounds.

The azimuthal segmentation of the A-B hodoscope array served two purposes. First, the A-B array which covered the upstream face of the toroid was employed as a muon hodoscope in coincidence with the muon hodoscopes, M and F, downstream of the toroid, to track the muon through the toroid and into the polarimeter. Detailed coincidences between the various azimuthal sectors of the muon hodoscope arrays were used to select events with a well-defined muon track remaining roughly within one octant (45°) of azimuth. Second, the azimuthal segmentation of the A-B

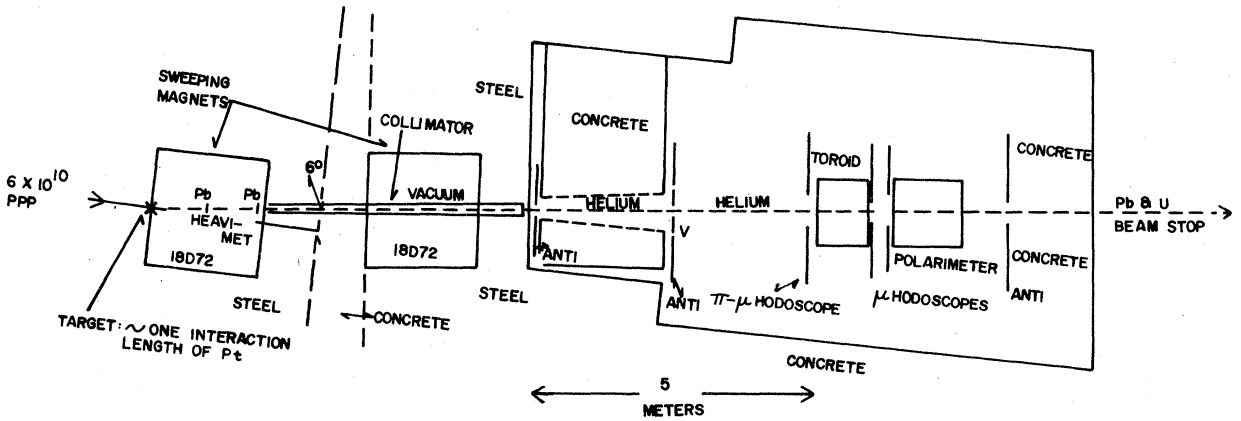

FIG. 5. Layout of the 6° neutral beam line.

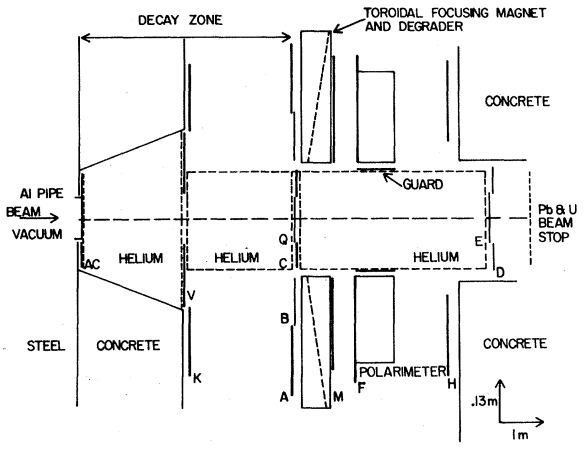

FIG. 6. A layout of the detector cave (note foreshortened scale) indicating the sizes and locations of the scintillation-counter arrays (*A*, *B*, *C*, etc.).

hodoscope was used to detect class-*M* events by requiring a pion hit in an *A*-*B* sector adjacent to the one defining the muon.

The class-*P* events were defined by the passage of the pion through one of the *C*, *D*, or *E* counters in coincidence with the muon. Pion trajectories very near the beam line were defined by coincidences of the counter *Q* with one of the *D* or *E* counters. With the exception of the *Q* and *E* counters, all counters in the experiment were made of 6.4-mm-thick NE 102 scintillator. The *Q* and *E* counters were 3.2 mm thick to reduce beam interactions as they were placed directly in the neutral beam.

The *V* array, located in the middle of the decay zone, was used logically as a single counter to aid in the detailed selection of events from the general *P* or *M* classes. Also, the *V* array "localized" the decay vertex aiding in a comparison of the event rates through various parts of the π-μ hodoscope with the Monte Carlo calculations.

The π-μ hodoscopes were each centered symmetrically on the beam line to ±1 mm and were all perpendicular to the beam line to ±10 mrad. There was no relative rotation of the arrays about the beam line to ±2 mrad.

D. Toroidal magnet

The toroidal magnet was designed to roughly focus positive muons into the polarimeter. The toroidal core was constructed with an increasing axial thickness as a function of radius. Uniform energy loss was afforded by a degrader, fashioned as a complementary plug, which was placed just downstream of the toroid core. Both the toroidal core and the degrader were constructed from 17.8-cm-thick machined laminations of 1010 steel. The toroidal core was wound with 704 turns of AWG No. 12 copper wire. To preserve the azimuthal character of the applied field the coil was wound with constant pitch, having half of the turns applied clockwise about the toroid axis, the other half counterclockwise. An average saturated field in the toroid of 15 kG was achieved by powering the coil with a direct current of 13 A. The toroid deflected negative muons from the beam line so that few stopped in the polarimeter.

The toroid-degrader assembly had an active volume extending from a radius of 17.8 to 61 cm; the hole provided a passage for the neutral beam. The length of the assembly was 71 cm, representing 0.56 kg/cm^2 of steel. A laboratory kinetic energy of $\gtrsim$825 MeV was then required for a muon to penetrate the toroid, and the mass (6000 kg) of the assembly shielded the polarimeter from the background of π's, e's, and γ's from K_L^0 decays occurring upstream.

E. Polarimeter

The polarimeter served two purposes in the experiment. As a degrader it tracked the muons as they were brought to rest, and as a polarization analyzer it detected the positron from the muon decay.

The polarimeter consisted of 32 wedge-shaped aluminum blocks distributed about a 40.6-cm-diameter stainless steel neutral beam pipe (Fig. 2). The blocks were covered on most faces with 6.4-mm-thick scintillation counters. With a mass of 47 kg each, the blocks were cast from No. 356 No Heat aluminum, and carefully machined to be symmetric. The active volume of the polarimeter extended from the neutral beam pipe to a radius of 53.3 cm. The polarimeter blocks were 91.4 cm long, representing 0.25 kg/cm^2 of aluminum. Muons with a range of energies between 825 and 1265 MeV were able to penetrate the toroid assembly and stop in the polarimeter.

The position, in azimuthal angle about the beam line, of the stopping muon was determined by the prompt (associated with the overall trigger) signals in the counters surrounding each block (Fig. 7). The large array *H* (Fig. 6) located immediately downstream of the polarimeter was set in anticoincidence to veto events in which the muon did not come to rest in the polarimeter. The upstream face of each block was covered by one *F* counter, which identified the muon's entry point. The *G* counters, covering the radial faces of the blocks, allowed the detection of any multiple scattering of the muon from one block to another.

The positron from the muon decay was detected as a delayed signal in one of the two *G* counters flanking the block in which the muon had stopped.

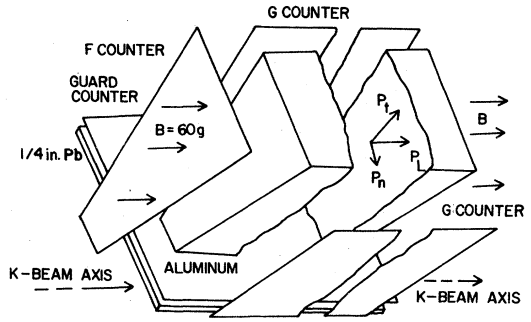

FIG. 7. An exploded view of the polarimeter section.

A set of guard counters were mounted along the inside of the polarimeter beam pipe and covered with 6.4 mm of lead. These were used to suppress the background contamination due to K_L^0 decays (including $K_L^0 \to 3\pi^0 \to 6\gamma$) occurring along the length of the polarimeter.

The flux of slow neutrons in the vicinity of the polarimeter was attenuated by placing the entire detector in a concrete cave which included a 46-cm-thick roof, and an additional 46-cm-thick wall upstream of the neutral beam stop.

The active volume of the polarimeter was subjected to a uniform magnetic field of 60 G directed along the polarimeter axis. A solenoidal coil with a diameter of 1.25 m was wound upon a form consisting of a plastic shell surrounding the polarimeter block assembly. The coil consisted of 482 turns of 3.2-mm × 3.2-mm copper wire. To preserve the axial character of the applied field, the coil was wound in two layers with an equal number of turns of equal but opposite pitch. Except for the neutral beam hole, the entire assembly was surrounded by a shell of 1010 steel, formed by two 12.7-mm-thick end plates connected by a 6.4-mm-thick cylinder. The shell served to return the magnetic flux from the solenoid, enhancing the uniformity of the field. It also acted as a magnetic shield, protecting the active polarimeter volume from stray external fields (e.g., the earth's field of 525 mG) and protecting the counter phototubes from stray fields due to the solenoid. With a current of 10 A in the solenoid coil, the axial field was measured to have a value of 60 G and was uniform over the active volume to ±2%. The field direction was reversed between beam pulses, once every 2.5 sec. The relaxation time constant for the solenoid was 0.08 sec guaranteeing the absence of transient fields during the 1-sec beam spill. The axial field was measured to have the same magnitude in both directions to ±30 mG.

The entire polarimeter assembly, with a mass of 2500 kg, was capable of being rotated about its axis, affording a means to study subtle systematic effects.

F. Electronics and data handling

The electronics and computer software for the experiment were carefully designed so that event selection and data analysis were accomplished in an on-line fashion. Several levels of data handling were required, but the overall design provided the convenience of monitoring the progress of the experiment in detail, a critical feature in a precision measurement. A schematic of the experimental logic is illustrated in Fig. 8.

Logically, the first level of data handling consisted of a fast (nanosecond timing) trigger generated by scintillation-counter coincidences. Throughout the apparatus Amperex 2230 photomultiplier tubes were used to view the counters, and the outputs were shaped for digital use by standard (LeCroy) discriminators. The fast trigger circuitry was built using Motorola ECL (emitter-coupled logic) series 10 000 logic gates, and was capable of operating upon signals with a width of 5 nsec. Specifically, the fast trigger performed the following functions:

(1) Muon hits in the A-B hodoscope were identified by the requirement of specific coincidences with the M and F hodoscopes. For example, the logical combination

$$A_\mu^1, B_\mu^1 \equiv (A_1 + A_2, B_1) \cdot [(F_{32} + F_1 + F_2) \cdot (M_8 + M_1) + (F_3 + F_4 + F_5) \cdot (M_1 + M_2)]$$

identified a muon in the azimuthal region of 0°–45°. The larger acceptance in the M array was chosen to avoid biasing, and the acceptance of the F array was set to be 67.5° to allow for multiple scattering in the toroid. Note that the 16 A counters were used logically in pairs.

(2) The event configuration, or "type", was determined by the complement of hits in the A, B, C, D, E, and V arrays, and was required to be one of the configurations selected by the Monte Carlo calculations. With muon hit defined as above, the allowed configurations are given in Table I.

(3) Anticoincidence counters AC, K, and H were used to veto the event at this level. The event was also vetoed by a shower of more than two hits in the A, B, C, D, and E arrays as determined by an analog adder.

The trigger was used as an initializing signal, indicating the beginning of an event. At the nominal beam intensity (6×10^{10} protons on target per pulse with a 1-sec beam spill) the fast trigger rate was about 80 per pulse.

The more cumbersome task of identifying the

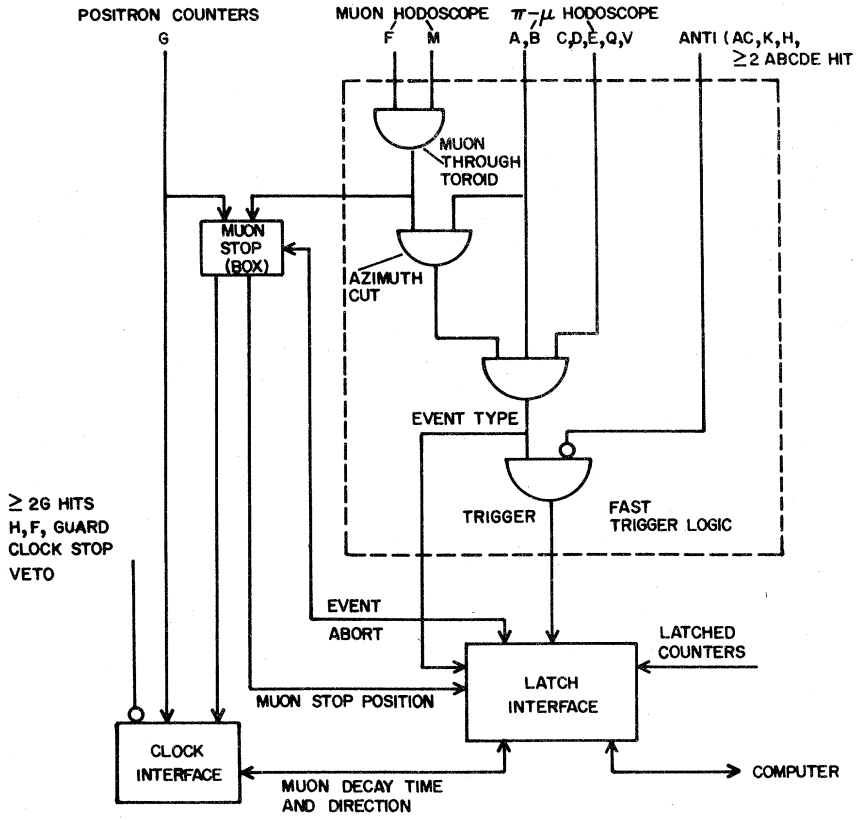

FIG. 8. A schematic overview of the experimental electronics.

TABLE I. Logical combinations of hits in the π-μ hodoscope for the allowed event configurations. $i=1,8$ cyclic. A_μ^i and B_μ^i are defined in the text.

P class events		*M* class events	
Type	Configuration	Type	Configuration
1	$B_\mu^i \cdot E_\pi \cdot \overline{V}$	10	$A_\mu^i \cdot (A^{i-1} + A^{i+1})_\pi \cdot V$
2	$B_\mu^i \circ D_\pi \cdot \overline{V}$	11	$B_\mu^i \cdot (B^{i-1} + B^{i+1})_\pi \cdot \overline{V}$
3	$A_\mu^i \cdot D_\pi \cdot \overline{V}$	12	$B_\mu^i \cdot (A^{i-1} + A^{i+1})_\pi \cdot \overline{V}$ [c]
4	$B_\mu^i \circ E_\pi \cdot V$	13	$B_\mu^i \cdot (A^{i-1} + A^{i+1})_\pi \circ V$ [c]
5	$B_\mu^i \cdot D_\pi \cdot V$		
6	$B_\mu^i \circ C_\pi$ [a] $\cdot V$		
7	$A_\mu^i \cdot E_\pi \circ V$		
8	$A_\mu^i \circ D_\pi \circ V$		
9	$A_\mu^i \circ C_\pi$ [b] $\circ V$		

[a] For type 6, *C* 1, 2, 3, 7, or 8 is allowed with B_μ^1.
[b] For type 9, *C* 1 is not allowed with A_μ^1.
[c] For types 12 and 13, a small (~10%) admixture of $A_\mu^i \circ (B^{i-1} + B^{i+1})_\pi$ is present due to multiple scattering in the toroid.

polarimeter block in which the muon had stopped was accomplished by a slower, transistor-transistor-logic (TTL) based circuit. The "box finder" was initialized by the trigger, and employed field-programmable logic arrays (FPLA) (Ref. 27) operating on prompt latched signals from the *F*, *M*, and *G* counter arrays. Each polarimeter block was surrounded by "box" consisting of one *F* (·*M*) counter and two *G* counters, and if only one of these three counters were hit, the muon was considered to have stopped in the block; if two counters were hit, the muon was presumed to have passed through the block. If the logic found no unambiguous stopping position (box) or more than one stopping position, the event was aborted. At nominal beam intensity about half of the fast triggers survived this logical requirement.

The clock interface[28] circuitry served to record the direction and time of the delayed muon decay event. Each *G* counter was associated with a clock, consisting of a 64-bit scaler which counted pulses from a 10-MHz crystal oscillator during the 6.4-μsec gate initialized by the fast trigger.

The decay positron, in passing through a G counter, would stop the associated clock recording the time of the decay to 100 nsec. Particles entering the polarimeter that were not associated with the trigger could also stop the clocks. This background could have caused a severe dilution of the signal. However, the nearly complete shell of counters surrounding each G counter, inherent to the geometry of the polarimeter, served as a useful anticoincidence in this regard: For a delayed hit in a given G counter, any other G hit or any hit in the F, H or guard counter arrays vetoed the clock stop. Although all of the clocks were started at the beginning of an event, only those two associated with the muon stopping block were interrogated by the latch interface.

The latch interface[29] served as the link between the detector electronics and the computer. Acting as a controller the latch interface accepted a signal from the fast trigger if a previous event was not in progress. At this time a signal was sent to the clock interface to start the clocks, and an array of latches (D flip-flops) were set to record the prompt event data. This information included the relevant counters hit, the event configuration, and the muon stop position. In order to monitor the backgrounds in the counter arrays, the latches were set again, to record counts 200 nsec after the trigger. When the 6.4-μsec decay gate was closed, the latch interface stored the information from the event, including the position and time of the decay, in a local $8k$ bit memory. The computer was then able to read data from this memory asynchronously. The local memory was cleared before each beam pulse.

The on-line analysis and compilation of data were performed by a PDP-11/40 computer. Among the more important data rejections dictated by the software were the following:

(i) Rejection of events with zero or two clock stops recorded for a given muon stop. For each stopping muon, the decay time and direction was unambiguously defined.

(ii) Rejection of events in which the muon traversed more than two G counters in coming to rest in the polarimeter.

(iii) Rejection of a subset of events from types 6 and 9 according to the detailed configuration of the B or A and C hits. (See notes in Table I.)

Roughly 25% of the processed events survived these criteria, and the recorded event rate was ~10 events per pulse.

With each beam pulse, the computer also received, via a CAMAC Dataway bus, the direction of the solenoid field (north or south), the beam intensity (protons on target), and scaler rates in the counter arrays (OR A's, OR G's, etc.). The analyzed data were stored on the disk, which provided two sources of useful summaries which could be examined while data were being accumulated. The first level contained histograms of the distribution of counter hits, the accumulated scaler readings and event rates, and was periodically updated (every 20 000 events), providing information on the variation of the experimental conditions over short (2 h) time scales. The second level of data storage contained the accumulated event statistics providing summaries and plots of the muon-decay time and the asymmetries as a function of time for the total sample of data and for the two main classes of events (P and M).

To augment the rich summary of data collected on-line, data tapes were written, recording the essential information for each event, for later off-line analysis. Specifically, the event type, the muon's entry point and stopping position in the polarimeter, the time and direction of the decay, the solenoid field direction, and the A-B octant hit were packed into two 16-bit words. These were written on tape in records of 1032 words, along with a summary of the experimental parameters (the time, beam intensity, scaler rates, etc.). About 1.5 million events were written on each tape, and the analysis of the ten tapes collected provided useful information concerning possible biases and systematic effects in the experiment.

IV. DATA ANALYSIS

A. General

The following analysis is based on 12×10^6 events collected with the apparatus set to accept the preferred sample of $K_{\mu3}$ decays. Another 2×10^6 events were collected under other conditions, in order to study systematic effects. Specifically, measurements were made with varying beam intensity, with a reversal of the toroid polarity and with a misalignment of the hodoscope arrays.

Monte Carlo calculations provided a useful guide for a comparison of the relative distribution and polarizations of the allowed event configurations. These calculations were dependent on the assumed K_L^0 momentum spectrum, which was generated by a modified form of the Sanford-Wang[30] parametrization. The acceptance of the apparatus, including the detector geometry and the trigger logic, was folded in by propagating the $K_{\mu3}$ decay products through the detector. The observed rates agreed well with the Monte Carlo estimates. For 10^{11} protons on target we expected about 50 000 K_L^0 decays (to $\pi^-\mu^+\nu_\mu$), in the 5-m drift space, from kaons with a momentum greater than

1.2 GeV/c. For the decaying kaons with a momentum greater than 1.2 GeV/c the spectrum behaves as $e^{-0.6P}$ (P in GeV/c). Of these decays about 2% had a valid muon stop in the polarimeter, and 6% of these were accompanied by the detection of a pion satisfying the trigger.

In propagating the muons through the toriod-degrader and into the polarimeter, processes resulting in an effective depolarization were taken into account. The muon polarization was calculated in laboratory coordinates, at the position of the kaon decay, using the Cabbibo and Maksymowicz[22] formula with $\xi = 0.0 + i0.01$. In general the muon spin direction was expected to follow the momentum for motion in the magnetic field of the toroid. However, nuclear Coulomb collisions resulted in a depolarization of about 5%.[31] In addition, multiple scattering and the dispersion of the focusing action of the toroid resulted in an effective further depolarization of about 10%.

Muons stopping in the polarimeter would have an entering energy of less than 500 MeV and would not be expected to suffer significant depolarization as they came to rest in the aluminum polarimeter blocks.[32] The Monte Carlo calculation was then terminated at the point where the muon entered the polarimeter. It is noted that the depolarization effects mentioned above do not generate a spurious T-violating signal and affect mainly the sensitivity of the polarimeter. The analyzing power for the polarimeter was not calculated as the computations required are more difficult and thus less reliable, especially since the analyzing power is known to be dependent on the detailed distributions of muons stopping in the aluminum wedges which we are unable to measure. The analyzing power was expected to be of ~0.20 based on previous measurements with aluminum polarimeters.[33]

The results of the Monte Carlo calculations are presented in Table II. For each configuration we list the expected percentage contribution to the event rate. Also presented are the expectations for the polarization components P_t and P_n as found in the kaon rest frame and in the laboratory.

B. Muon-decay distribution

The events with polarimeter clock stops were due largely to the detection of positrons from μ^+ decay. However, contributions from μ^- decays and random backgrounds were expected and accounted for by parametrizing the total time variation of the delayed event distribution as

$$I(t) = e^{-\gamma_B t}(N^+ e^{-t/\tau^+} + N^- e^{-t/\tau^-} + B) .$$

Here $N^\pm$ are the normalized amplitudes for the $\mu^\pm$ contributions, and $\tau^\pm$ are the lifetimes for muons in aluminum (2.198 μsec for μ^+ and 0.88 μsec for μ^-), B is the background level, and γ_B is the background frequency.

A least-squares fit to the entire data sample was made using the above distribution and the FUMILI fitting routine. The results suggest that, integrating over the 6.4-μsec decay gate, the delayed events were composed of 64% μ^+ decays, 2% μ^-

TABLE II. Monte Carlo expectations for relative rates and polarizations of the allowed event configurations; $\mathrm{Re}\xi = 0.0$, $\mathrm{Im}\xi = 0.01$.

Type	Configuration	Events (%)	$\langle P_t^{\mathrm{c.m.}} \rangle$	$\langle P_n^{\mathrm{c.m.}} \rangle$ (%)	$\langle P_t^{\mathrm{lab}} \rangle$	$\langle P_n^{\mathrm{lab}} \rangle$ (%)
1	$BE\bar{V}$	4.7	0.78	0.30	0.67	0.26
2	$BD\bar{V}$	19.7	0.72	0.29	0.65	0.20
3	$AD\bar{V}$	2.2	0.79	0.38	0.60	0.30
4	BEV	1.7	0.80	0.18	0.61	0.14
5	BDV	2.6	0.76	0.18	0.64	0.16
6	BCV	4.8	0.87	0.21	0.29	0.12
7	AEV	3.1	0.81	0.32	0.72	0.24
8	ADV	5.1	0.76	0.30	0.70	0.23
9	ACV	21.4	0.68	0.28	0.68	0.15
10	AAV	9.6	0.90	0.30	−0.49	−0.16
11	$BB\bar{V}$	7.7	0.90	0.30	−0.49	−0.17
12	$BA\bar{V}$	3.7	0.91	0.32	−0.48	−0.24
13	BAV	13.8	0.87	0.24	−0.47	−0.14
P	$\sum$(Nos. 1–9)	65.2	0.738	0.288	0.640	0.198
M	$\sum$(Nos. 10–13)	34.8	0.891	0.283	−0.484	-0.169
Total	$\sum[P + (-1)M]$	100.0	0.795	0.286	0.586	0.187

decays, and 34% random clock stops. The μ^- fraction is to be considered an estimate, because the fraction of muons stopping in scintillator is uncertain and thus the effective lifetime of the μ^- sample is uncertain.

The clock-stop rate due to random backgrounds was the limiting factor in the data collection rate. For the nominal beam intensity of 6×10^{10} protons per pulse on target, the counting rate in the 32 positron counters was about 250 kHz. For a single G counter the rate was about 50 kHz of which nearly 60% could be accounted for as being due to charged particle and photon fluxes entering the active polarimeter volume. These fluxes were effectively removed by the anticoincidence logic associated with the clocks. However, the remaining "neutral" flux then accounted for the observed fraction of accidental clock stops occurring during the 6.4-μsec decay gate. The origin of the neutral flux was poorly understood, although it was thought to be largely the result of γ rays emitted in the course of neutron capture in ^{27}Al and β and γ rays from the decay of ^{28}Al. The ^{28}Al decays were, in fact, observed. We note that in a special test using two 3.2-mm-thick counters in coincidence in place of the usual 6.4-mm-thick positron counter, the effective background rate decreased by a factor of 4, implying a factor of 2 gained in allowable beam intensity.

C. Muon-decay asymmetry

The components of muon polarization were determined by the analysis of the time variation of the asymmetry $A=(U-D)/(U+D)$ in the positron counters. The cylindrical symmetry of the polarimeter, both in geometry and efficiency, allowed the data from all 32 polarimeter sections to be combined with identical weights. In the following, U is the intensity of positrons detected in the counter located on the clockwise side of any polarimeter block; D is the intensity on the counterclockwise side:

$$U_{\pm}(t)=e^{-\gamma_B t}\{N^+[1+\alpha\cos(\pm\omega t+\phi_0^U)]e^{-t/\tau^+}+N^-e^{-t/\tau^-}+B\},$$

$$D_{\pm}(t)=e^{-\gamma_B t}\{N^+[1+\alpha\cos(\pm\omega t+\phi_0^D)]e^{-t/\tau^+}+N^-e^{-t/\tau^-}+B\},$$

where the subscript $\pm$ indicates the axial field direction and thus the sense of muon spin precession (+ for the field directed upstream, and the μ^+ spin precessing clockwise about the beam axis); the precession frequency $\omega=g_{\mu e}|\vec{B}|/2m_\mu c$ and the amplitude $\alpha=\eta|\vec{S}_\perp|$, where η is the analyzing power and $|\vec{S}_\perp|$ is the polarization amplitude normal to the axis of precession. Note that ϕ_0 is the initial azimuthal angle of the muon spin about the beam axis, as measured from the vector normal to the detector (U or D.)

As indicated in Fig. 9, it is evident that the T-conserving polarization P_t is initially parallel to the plane bisecting the polarimeter section, and $\phi_0\cong\pm\pi/2$ (+ for the D counter, − for the U counter). Thus, taking the axial field direction into account, the T-conserving asymmetry is calculated to be

$$A_t(t)=\frac{(U_+-D_+)-(U_--D_-)}{U_++D_++U_-+D_-}=[A_t(0)/C(t)]\sin\omega t,$$

with

$$C(t)=1+(N^-/N^+)e^{t(1/\tau^+-1/\tau^-)}+(B/N^+)e^{t/\tau^+},$$

and

$$A_t(0)=\eta P_t,$$

where η is the analyzing power. Also note that $t=t_{\text{measured}}+t_0$, with t_0 being the instrumental phase shift. Similarly for the T-violating component P_n, $\phi_0\cong0$ (for the U counter) or π (for the D counter) and the T-violating asymmetry is calculated to be

$$A_n(t)=\frac{(U_+-D_+)+(U_--D_-)}{U_++D_++U_-+D_-}=[A_n(0)/C(t)]\cos\omega t,$$

with $C(t)$ as above and $A_n(0)=\eta P_n$.

In the above formulation the implicit assumption has been made that the background contributions to the intensities in the U and D counters are symmetric. Also, the negative muons are not expected to contribute to the asymmetry as they, unlike positive muons, are rapidly depolarized after coming to rest in the aluminum polarimeter.[34]

In Fig. 10 the measured asymmetries A_t and A_n are plotted as a function of time for the P and M event classes and the total event sample. The asymmetries for the total event sample are obtained by algebraically summing the contributions from the P and M event classes, but multiplying

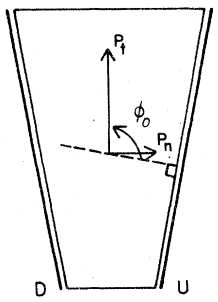

FIG. 9. A definition of ϕ_0, the initial azimuthal angle of the muon polarization (component) about the beam axis as measured from the normal to a positron counter (U or D).

the contribution from the M class by -1 to account for the expected and observed difference in sign.

As expected, the T-conserving component A_t clearly exhibits a sinusoidal form, and the decreasing amplitude is due to the background dilution manifest in the factor $C(t)$ in the above parametrization. A least-squares fit to A_t for the entire event sample yielded $\omega = 5.21\ (\mu\text{sec})^{-1}$, in agreement with the measured value of the axial precession field. Also, t_0 was determined to be 0.055 μsec, consistent with independent measurements on the clock electronics.

In addition, the fitted values for the asymmetry amplitudes, $A_t(0)$ and $A_n(0)$, are given. For the total data sample $A_t(0) = 0.0513 \pm 0.0007$ implying a measured value for the T conserving transverse polarization $P_t^{\text{lab}} = 0.417 \pm 0.063$, where a value for the effective analyzing power $\eta = 0.12 \pm 0.02$ was used, based on detailed analysis of the asymmetries predicted and observed for the 13 event types. For the T-violating transverse polarization a value $P_n^{\text{lab}} = 0.0017 \pm 0.0056$ is obtained from the asymmetry $A_n(0) = 0.000\,21 \pm 0.000\,69$ and is seen to be consistent with zero, and thus with time-reversal invariance.

Noting that the precession period is $T = 1.2$ μsec and that the asymmetry data were collected in 0.1-μsec time bins, it was convenient to Fourier analyze the data with respect to the precession frequency. With the background subtracted, the data from the first 60 time bins were collapsed into 12 bins, representing data points in one cycle period separated by equal intervals of phase. Because instrumental asymmetries were found to occur in the first time bin these points have not been plotted and were not included in the analysis. The folded asymmetry data are plotted on the right in Fig. 10. The $\sin\omega t$ behavior of the A_t plots is in each case again obvious, and the lack of $\cos\omega t$ dependence in the A_n plots is also clear. A least-squares fit for the asymmetry amplitudes was made with the instrumental phase shift t_0 set from the previous fits.

The results of the analysis for the folded data are presented in Table III. Besides the asymmetry amplitudes $A_t(0)$ and $A_n(0)$, the number of events collected and the effective number of events collected (that is, with the background subtracted) are listed. Results are presented for each of the allowed event configurations (types 1–13) as well as for the P and M event classes and the total event sample. We note that the T-violating asymmetry is consistent with zero for each event type, thus indicating an absence of large systematic errors.

In a detailed comparison of the results with the Monte Carlo predictions, events of types 6, 9, and 12 are noted to have relatively smaller T-conserving asymmetry amplitudes. The reduced sensitivity is correlated with a larger relative dilution due to backgrounds. This is found in comparing the number of effective events to the collected events, and in comparing the number of collected events to the relative number of events expected from the Monte Carlo. The origins of the backgrounds for these event types were investigated, and some sources were understood so that a fraction of events have been eliminated by further constraints implemented in the course of the experiment, all of which are reflected in Table III. It is noted that type 9 is the major contributor to the discrepancies in the relative number of events predicted and observed.

Comparisons of the data and the Monte Carlo also allowed an approximate determination of the value of $\text{Re}\xi$. The ratio of events and the ratio of the magnitudes of the T-conserving transverse polarizations for the P and M event classes were compared to the ratios predicted by the Monte Carlo for various values of $\text{Re}\xi$. The results support the conclusion that $\text{Re}\xi$ is small and negative. It is noted that the determination of $\text{Re}\xi$ depends strongly on the details of the Monte Carlo calculations. However, due to the geometry and acceptance of the detector and the event selection criteria, the determination of $\text{Im}\xi$ is relatively insensitive to variations in the calculations.

D. Backgrounds

The contamination of the $K_{\mu 3}$ sample by events of other origins was small due to the complexity of the trigger. Random triggers due to coincidences between unassociated particles were suppressed by the requirements of exactly two particles in the π-μ hodoscope and a well defined muon track through the toroid. Specifically the $>2ABCDE$ veto reduced the trigger rate by 30%, thus removing ambiguous high multiplicity events. Also, the muon hodoscope array M was found to reduce the trigger rate by 25% effectively removing the contributions due to decay particles originating upstream of the polarimeter, including those from the hole in the toroid.

In any event, real or background, a genuine muon track was required. However, a π^+ decay upstream of the toroid could satisfy the requirement. The prominent K_L^0 decay modes $K_L^0 \to \pi^-\pi^+\pi^0$, $\pi^+\mu^-\bar{\nu}_\mu, \pi^+e^-\bar{\nu}_e$ could contribute in this manner especially if the negative particle in each case mimicked the π^- normally detected in the decay $K_L^0 \to \pi^-\mu^+\nu_\mu$. However, the muon from the pion decay would be required to have the appropriate

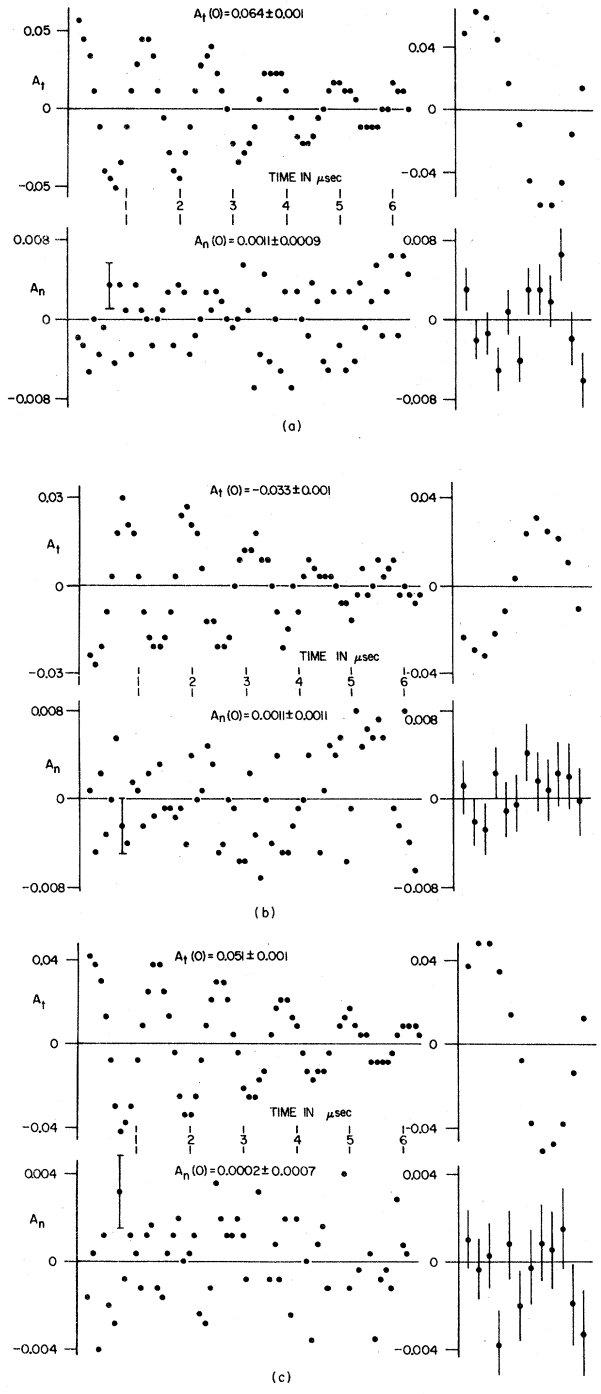

FIG. 10. Plots of the muon-decay asymmetry as a function of time. The upper curves are for the T-conserving asymmetry A_t while the lower curves are for the T-violating asymmetry A_n. On the right are plots of the asymmetry for the same data, with the background subtracted, modulo the precession period of 1.2 μsec. (a) P class events, (b) M class events, (c) total data sample.

transverse momentum and energy for passage through the toroid-degrader. Calculations imply that less than 3% of the π^+ decays from these various K_L^0 decay modes could be misidentified as a muon.

Another source of muons were high-energy pions decaying between the target and the proton beam stop. The flux of such penetrating muons was largely removed by the anticoincidence arrays AC and K which reduced the trigger rate by 25%. An estimate of the remaining contribution of this source to the event rate is based on the knowledge that $K_{\mu 3}$ decays would give symmetric distributions in the π-μ hodoscope arrays. This assumes that the counters were equally efficient, as they were monitored to be, and ignores the small variations in intensity due to the finite acceptance in production angle of the K_L^0 beam. However, the K_L^0 beam, the proton beam, and the sweeping magnets form a plane which breaks the cylindrical symmetry. We expected and found the high-energy muon flux to be mostly in this plane. Then, even with the anticoincidence counters, we found a nonsymmetric distribution in the hodoscopes implying a background of approximately 7%.

It is also noted that the trigger logic and software were designed to reject events in which it was possible for a single unvetoed muon to pass through an A (or B) scintillation counter and then through the light pipe of a B (or C) counter ($\beta = 0.67$ for light in lucite).

With the above considerations we estimate that the contribution to the event sample due to background sources is approximately 10–15%. The effect of these background events is to reduce the effective sensitivity of the polarimeter as the muons involved are mostly longitudinally polarized, which is equivalent to being unpolarized in our polarimeter. In no way can the various backgrounds cause a spurious T-violating signal.

E. Systematic errors

An instrumental asymmetry defining a net screw sense in the detection of muon decays with respect to the laboratory $K_{\mu 3}$ decay plane will result in a systematic error in P_n and a false T-violating effect. In the following we review possible sources of such errors and the measures taken to reduce and monitor the effects.

Many of the sources for systematic errors in P_n are the result of an effective rotation of the nonzero transverse polarization component P_t out of the plane bisecting a polarimeter section. Figure 11 illustrates this effect schematically. Muons are expected to be uniformly distributed in the counter B and then in the polarimeter sec-

TABLE III. Summary of the experimental results including event totals and results from the least-squares analysis of the asymmetry amplitudes.

Type	Configuration	$10^{-3}\times$ events (raw)	$10^{-3}\times$ events (less background)	$A_t(0)$	$A_n(0)$	Statistical error
1	$BE\bar{V}$	648	433	0.0729	0.002 17	0.002 74
2	$BD\bar{V}$	1 906	1286	0.0710	−0.000 55	0.001 59
3	$AD\bar{V}$	204	126	0.0644	−0.000 79	0.005 20
4	BEV	377	216	0.0504	−0.000 27	0.004 08
5	BDV	765	430	0.0535	−0.002 69	0.002 91
6	BCV	762	365	0.0132	0.006 90	0.003 28
7	AEV	354	264	0.0880	0.002 69	0.003 36
8	ADV	788	590	0.0839	0.004 86	0.002 24
9	ACV	642	405	0.0557	−0.001 94	0.002 88
10	AAV	1 034	705	−0.0377	−0.001 01	0.002 13
11	$BB\bar{V}$	1 115	731	−0.0321	0.001 12	0.002 12
12	$BA\bar{V}$	661	359	−0.0208	0.003 51	0.003 21
13	BAV	1 662	1049	−0.0345	0.001 68	0.001 80
P	$\sum$(Nos. 1–9)	6 445	4126	0.0639	0.001 12	0.000 90
M	$\sum$(Nos. 10–13)	4 470	2846	−0.0329	0.001 11	0.001 09
Total	$\sum[P+(-1)M]$	10 915	6971	0.0513	0.000 21	0.000 69

tion F. The associated pions are expected to be uniformly distributed in either of the two A counters. Even in the absence of CP violation (or final-state interactions), events with the pion detected on the right will have a nonzero component of muon polarization normal to the symmetry plane, since the decay plane in the kaon rest frame does not lie in the symmetry plane. Events with the pion on the left will, however, have an equal but opposite component of polarization and, if detected in equal numbers, the contamination of P_n due to P_t is in principle eliminated. However, in practice this cancellation depends on the cylindrical symmetry in terms of construction, placement, and efficiency of the π-μ hodoscope counters, and the freedom from relative rotations among the π-μ hodoscope arrays and the polarimeter. By design the deviations from this required symmetry were maintained so that the effective net angle of rotation was less than 2 mrad and then the systematic error in P_n was less than 0.001, and thus negligible with respect to the statistical error.

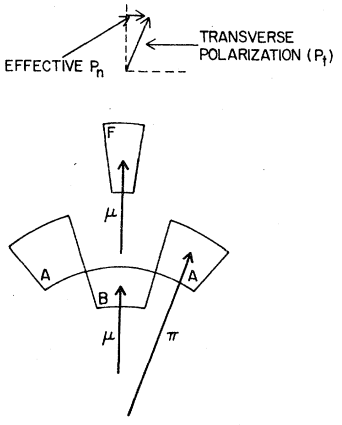

FIG. 11. A Schematic representation of an event indicating the potential systematic contribution of the T-conserving polarization component P_t to the T-violating polarization P_n.

The use of a reversing axial precession field in analyzing the muon polarization offered considerable freedom from systematic errors due to possible asymmetries in the polarimeter detection efficiency. However, in order to avoid systematic effects associated with the screw sense generated by the current generating the field, it was necessary to maintain equality in the overall efficiency of the detector for the two field directions. Most importantly a difference in the magnitude of the axial field in the normal and reversed directions will lead to a contamination of the P_n data (behaving as $P_n\cos\omega t$) by a term $P_t\cos\omega t\times\sin\Delta\omega t$, where $\Delta\omega$ is the difference in the precession frequencies for the two field directions. Measurements of the field magnitude determined that $\Delta\omega/\omega\lesssim 5\times10^{-4}$, limiting the contribution to P_n to be about 0.002. In addition, the number of events collected with the field in the two directions was required to be the same to 0.1%. The leakage of flux from the solenoid end plates was sufficient to induce fields (3 G) at the positron counter (G)

phototubes so that the counter efficiency depended on the field direction. The effect was removed by placing a large bucking coil (1 m diameter, 80 turns, 10 A) in the plane bisecting the length of the phototubes.

We know of no other sources for screwlike asymmetries, except perhaps for the case of pathologically coordinated linear asymmetries which can simulate a screw sense. For instance, a screwlike asymmetry of about 10^{-4} could be generated by the effect of a 1% up-down asymmetry in the trigger coupled with 1% left-right asymmetry in the positron detection efficiency. Such asymmetries were monitored in the course of the experiment, and were found to contribute negligibly to the final result.

V. RESULTS AND CONCLUSIONS

The asymmetry results for the total data sample are used to obtain limits set by the experiment on the violation of time-reversal invariance. The mean value of the component of muon polarization transverse to the laboratory decay plane was measured to be $P_n^{\rm lab} = 0.0017 \pm 0.0056$. From the Monte Carlo calculations $\langle P_n^{\rm lab}\rangle = 0.187\%$ for $\mathrm{Im}\xi = 0.01$, so that $\mathrm{Im}\xi = P_n^{\rm lab}/0.187 = 0.009 \pm 0.030$. This result is to be compared with the value of $\mathrm{Im}\xi \simeq 0.008$ expected from the final-state interactions, and the values of $\mathrm{Im}\xi$ in the range of 0.001–0.01 expected from milliweak models of CP violation.

Even in the absence of specific predictions, the limits set on T-violating processes in weak decays are useful if considered in terms of the complex phase in the interference between two normalized amplitudes describing the decay. If CP violation is milliweak in character then one expects this complex phase to be related to the characteristic strength of CP violation given by $\epsilon = 2.3 \times 10^{-3}$. Thus $\phi_{CP} \sim 0.13°$.

For example, in nuclear β decay a T-violating effect would be the result of a complex interference between the Fermi and the Gamow-Teller transition amplitudes. The T-odd correlation measured is $D\hat{S}_N \cdot (\vec{p}_e \times \vec{p}_\nu)$, where $\hat{S}_N$ is the initial nuclear polarization. The present values for the parameter D are from ^{19}Ne decay, $D = -0.0005 \pm 0.0010$,[6] and from neutron β decay, $D = 0.0022 \pm 0.0030$.[35] These values imply that the complex phase angle has a value of $\phi = (179.94 \pm 0.11)°$ and $(179.71 \pm 0.39)°$, respectively, to be compared with the value 180° expected if time-reversal invariance is valid.

For $K_{\mu 3}$ decays we have shown in Sec. II A that the corresponding CP-violating phase angle is given by the average value of P_n/P_t evaluated in the kaon rest frame. From the Monte Carlo calculations we expect $\langle P_n^{\rm lab}\rangle = 0.187\%$, $\langle P_n^{\rm c.m.}\rangle = 0.286\%$, $\langle P_t^{\rm lab}\rangle = 0.586$, and $\langle P_t^{\rm c.m.}\rangle = 0.795$. With the measured values for the T-conserving and T-violating asymmetries, $A_t = 0.0513 \pm 0.0007$ and $A_n = 0.000\,21 \pm 0.000\,69$, the phase angle is given by

$$\phi = (286/187)(0.586/0.795)(A_n/A_t)$$
$$= 0.005 \pm 0.015$$

or $\phi = (0.26 \pm 0.86)°$. This we believe is the best measure of the sensitivity of the experiment. In the future we will begin similar measurements on $K^+_{\mu 3}$ decays. An improved sensitivity and the absence of final-state interactions will allow us to make measurements capable of detecting a milliweak CP-violating effect.

ACKNOWLEDGMENTS

We wish to thank the staff of the Brookhaven AGS for the close support and cooperation which made the experiment possible. One of the authors (M.P.S.) acknowledges the hospitality of the University of Pennsylvania Physics Department while this report was being written. This research was supported in part by the U. S. Department of Energy under Contract No. EY-76-C-02-0016.

---

*Submitted in partial fulfillment of the requirements for the degree of Doctor of Philosophy at Yale University.

[1] J. H. Christenson, J. W. Cronin, V. L. Fitch, and R. Turlay, Phys. Rev. Lett. 13, 138 (1964).

[2] K. Kleinknecht, Ann. Rev. Nucl. Sci. 29, 1 (1976); E. Paul, *Springer Tracts in Modern Physics* (Springer, New York, 1976), Vol. 79, p. 53.

[3] L. Wolfenstein, Phys. Rev. Lett. 13, 562 (1964).

[4] K. R. Schubert *et al.*, Phys. Lett. 31B, 662 (1970).

[5] W. B. Dress *et al.*, Phys. Rev. D 15, 9 (1977).

[6] R. M. Baltrusaitis and F. P. Calaprice, Phys. Rev. Lett. 38, 464 (1977).

[7] J. Sandweiss, J. Sunderland, W. Turner, W. Willis, and L. Keller, Phys. Rev. Lett. 30, 1002 (1973).

[8] R. N. Mohapatra, in *Proceedings of the 19th International Conference on High Energy Physics, Tokyo, 1978,* edited by S. Homma, M. Kawaguchi, and H. Miyazawa (Phys. Soc. of Japan, Tokyo, 1979), p. 604; H. Harari, Phys. Rep. 42C, 235 (1978).

[9] M. L. Perl *et al.*, Phys. Rev. Lett. 35, 1489 (1975).

[10]J. Ellis, in *Weak Interactions—Present and Future*, proceedings of SLAC Summer Institute on Particle Physics, 1978, edited by M. C. Zipf, (SLAC, Stanford, 1978).
[11]S. W. Herb *et al.*, Phys. Rev. Lett. 39, 252 (1977).
[12]M. Kobayashi and T. Maskawa, Prog. of Theor. Phys. 49, 652 (1973).
[13]F. J. Gilman and M. B. Wise, Phys. Lett. 83B, 83 (1979).
[14]B. F. Morel, Nucl. Phys. B157, 23 (1979); E. P. Shabilin, Yad. Fiz. 28, 151 (1978) [Sov. J. Nucl. Phys. 28, 75 (1978)]; B. W. Lee, Phys. Rev. D 15, 3394 (1977); J. Ellis, M. K. Gaillard, and D. V. Nanopoulos, Nucl. Phys. B109, 213 (1976).
[15]S. Weinberg, Phys. Rev. Lett. 37, 657 (1976); see also T. D. Lee, Phys. Rep. 9C, 143 (1974); A. B. Lahanas and N. J. Papadopoulos, Lett. Nuovo Cimento 18, 123 (1977); B. C. Unal, University of Heidelberg report, 1976 (unpublished); A. B. Lahanas and C. E. Vayonakis, Phys. Rev. D 19, 2158 (1979).
[16]A. A. Anselm and D. I. D'Yakonov, Nucl. Phys. B145, 271 (1978).
[17]M. P. Schmidt *et al.*, Phys. Rev. Lett. 43, 556 (1979).
[18]We adhere to the conventions of E. D. Commins, *Weak Interactions* (McGraw-Hill, New York, 1973).
[19]L. M. Chounet, J. M. Gaillard, and M. K. Gaillard, Phys. Rep. 4C, 199 (1972), p. 264; J. Lemonne *et al.*, Universities of Brussels report, 1976 (unpublished), p. 114.
[20]T. D. Lee and C. S. Wu, Ann. Rev. Nucl. Sci. 16, 476 (1966).
[21]S. W. MacDowell, Nuovo Cimento 9, 258 (1958).
[22]N. Cabibbo and A. Maksymowicz, Phys. Lett. 9, 352 (1964); 11, 360 (1964); 14, 72 (1966).
[23] E. S. Ginsberg and J. Smith, Phys. Rev. D 8, 3887 (1973); N. Byers, S. W. MacDowell, and C. N. Yang, in *Proceedings of the International Seminar in High Energy Physics and Elementary Particles, Trieste, 1965* (International Atomic Energy Agency, Vienna, 1965), p. 953 and private communication.
[24]M. Longo *et al.*, Phys. Rev. Lett. 18, 806 (1967); Phys. Rev. 181, (1969); D. Bartlett *et al.*, Phys. Rev. Lett. 16, 282 (1966).
[25]A detailed account of the Sandweiss experiment is given by W. C. Turner, doctoral thesis, Yale University, 1973 (unpublished).
[26]A. R. Clark *et al.*, Phys. Rev. D 15, 553 (1977); G. Donaldson *et al.*, Phys. Rev. Lett. 31, 337 (1973).
[27]W. Morse *et al.*, Rev. Sci. Instrum. (to be published).
[28]M. J. Lauterbach, doctoral thesis, Yale University, 1977 (unpublished), p. 44.
[29]D. M. Grannan, doctoral thesis, Yale University, 1978 (unpublished), p. 105.
[30]J. R. Sanford and C. L. Wang, Brookhaven National Laboratory AGS Internal Report, 1967 (unpublished).
[31]S. Hayakawa, Phys. Rev. 108, 1533 (1957).
[32]A. Buhler *et al.*, Nuovo Cimento 39, 824 (1965).
[33]C. M. Ankenbrandt *et al.*, Phys. Rev. 30, 2582 (1971).
[34]A. O. Weissenberg, *Muons* (North-Holland, Amsterdam, 1967).
[35]B. G. Erozolimskii *et al.*, Yad. Fiz. 28, 98 (1978) [Sov. J. Nucl. Phys. 28, 48 (1978)].